GEOLOGICAL SURVEY OF CANADA

OPEN FILE 5393

Gamma-Ray Gradiometry for Point-source Location

L.E. Sinclair, J.M. Carson, P.R.B. Saull

2006

Natural Resources Canada Ressources naturelles Canada

Canada

GEOLOGICAL SURVEY OF CANADA
OPEN FILE 5393

Gamma-Ray Gradiometry for Point-source Location

L.E. Sinclair, J.M. Carson, P.R.B. Saull

2006

©Her Majesty the Queen in Right of Canada 2006
Available from
Geological Survey of Canada
601 Booth Street
Ottawa, Ontario K1A 0E8

Sinclair, L.E., Carson, J.M., Saull, P.R.B.
2006: Gamma-Ray Gradiometry for Point-source Location,
Geological Survey of Canada, Open File 5393, 16p.

Open files are products that have not gone through the GSC formal publication process

Contents

1 Introduction **1**

2 Method **2**

3 Experimental Setup **2**

4 Raw Spectra **3**

5 Analysis **5**

5.1 Pulse pile-up correction 5

5.2 Systematic uncertanties 6

5.3 Distance reconstruction 7

6 Results **7**

6.1 Many five-second datasets 8

6.2 The left side 10

7 Discussion and Conclusions **11**

Gamma-Ray Gradiometry for Point-source Location

L.E. Sinclair[1], J.M. Carson[1], P.R.B. Saull[2]

[1] *Geological Survey of Canada, Earth Sciences Sector, Natural Resources Canada, 601 Booth St, Ottawa, K1A 0E8*
[2] *Institute for National Measurement Standards, National Research Council, 1200 Montreal Rd, Bldg M-35, Ottawa, K1A 0R6*

Abstract

A method to extract the location of a point source, from the counts obtained by two gamma-ray detectors at different distances from the source, has been developed. With two 4 litre NaI crystals at a separation of approximately 2 m from each other, only a few seconds of data are necessary to reconstruct the distance with a precision of better than about 20%, to a 600 μCi ^{137}Cs source, up to 10 m away.

1 Introduction

The Radiation Geophysics Section of the Geological Survey of Canada performs gamma-ray spectrometry surveys for use in locating and mapping radioactive contamination from both intentional and accidental releases [1, 2]. With the systematic coverage provided by an airborne survey, the team has a proven capability in locating a point source on the ground [3]. Given the source location, a rough estimate of source strength is also obtainable. This kind of information is crucial to ground crews entering a contaminated area to remove a radioactive source.

There are instances in which a truck-borne survey may be more feasible than an aerial survey. However, when the survey equipment is confined to a road, the peak count intensity does not correspond to the location of the source, which is located at some unknown distance to the right or left of the road.

There is an established method to determine distance to a point-source using a single detector which is moving with respect to the source. This method has found application in portal-detectors [4]. We have developed a complementary method for point-source location which relies on a multi-detector arrangement which can be stationary with respect to the source.

This paper presents a gradiometric method to obtain the distance to a point source using a dual-detector system. The results obtained by application of the method for a 600 μCi ^{137}Cs source and a 60 μ Ci ^{60}Co source are presented, as a function of source distance.

2 Method

For a gamma-ray detector A, of acceptance $\mathcal{A}_\mathrm{A}$ and efficiency ϵ_A, the number of counts per second, C_A, due to a source of activity S at a distance of R_A is,

$$C_\mathrm{A} = \frac{\mathcal{A}_\mathrm{A}\epsilon_\mathrm{A}S}{4\pi R_\mathrm{A}^2}, \tag{1}$$

where the attenuation in air has been neglected. If we have a second detector, B, we can form the ratio of the count rates,

$$\frac{C_\mathrm{A}}{C_\mathrm{B}} = \frac{\mathcal{A}_\mathrm{A}\epsilon_\mathrm{A}R_\mathrm{B}^2}{\mathcal{A}_\mathrm{B}\epsilon_\mathrm{B}R_\mathrm{A}^2}, \tag{2}$$

in which the source activity S, cancels.

If acceptance and efficiency of the two detectors are equal, this reduces to

$$\frac{C_\mathrm{A}}{C_\mathrm{B}} = \frac{R_\mathrm{B}^2}{R_\mathrm{A}^2}. \tag{3}$$

Let us assume that the detectors and the source are arranged as shown in Fig. 1. Inverting Eqn. 3, we arrive

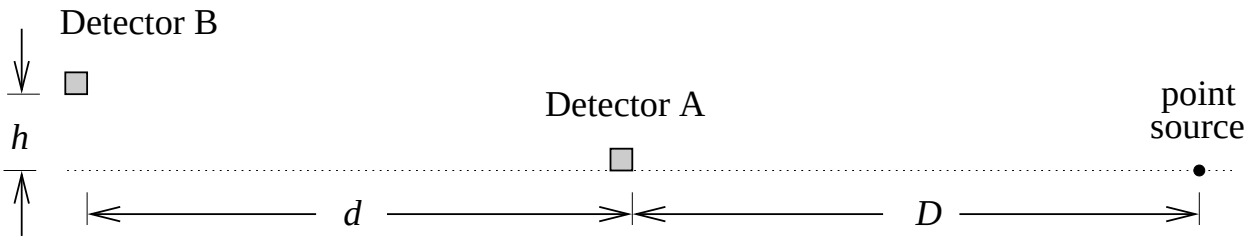

Figure 1: Experimental setup.

at the following expression for the distance of the source to detector A,

$$D = \frac{d + \sqrt{(d^2 + h^2)C_\mathrm{A}/C_\mathrm{B} - h^2}}{C_\mathrm{A}/C_\mathrm{B} - 1}. \tag{4}$$

Here, we have made the implicit assumption that detector A does not obscure detector B.

Thus, the method to reconstruct source distance using two detectors is simply,

1. Form the ratio of the count rates obtained with the two detectors after a suitable counting period, and
2. Extract the distance to the source from one of the detectors using Eqn. 4 (or similar, depending on the geometry of the setup).

3 Experimental Setup

The experiment took place at the National Research Council (NRC) in a large, low-scatter room of approximate dimension $16 \times 16 \times 10$ m with walls made of concrete.

The sources used were an encapsulated 600 μCi VIII-25 ^{137}Cs source and an encapsulated 60 μCi VI-20 ^{60}Co source, each with an active volume of less than 1 cm^3.

The detector system used was an SAIC Exploranium GR-460 system operating in dual-detector mode with two 4 litre NaI crystals. The crystals are rectilinear with dimensions $10.16 \times 10.16 \times 40.64$ cm^3. The spectrometer output one 512-channel spectrum over the energy range of 0 to 3 MeV, per detector, per second. Dead-times ranged from about 50 μs/s for a background run, to as much as 350 μs/s for a high-rate run. A correction for pile-up effects in the high-rate runs was performed (see Sec. 5.1).

The detectors were arranged as indicated in Fig. 1, with $d = 2.0$ m and $h = 0.3$ m. Detector A sat on the floor. Detector B sat on some blocks containing wax. The point source sat on the floor, horizontally in line with the centres of the sensitive volumes of the detectors. The detectors were oriented with their long side perpendicular to the line between the detectors and the source. Distances D were chosen to assure that no part of the front face of Detector B was obscured by its support blocks, and that Detector B was not shielded by Detector A.

Table 1 shows the distances at which runs were taken, and their durations.

	D: (m)	Duration: (s)
background		
	–	1648
600 μCi ^{137}Cs source		
	1.5	186
	2.0	182
	3.0	249
	5.0	226
	7.0	279
	10.0	487
	13.0	582
	15.0	700
	16.0	709
60 μCi ^{60}Co source		
	1.5	241
	2.0	436
	3.0	542
	5.0	349
	7.0	434
	10.0	676

Table 1: Run distances and durations.

4 Raw Spectra

The raw spectra obtained with the ^{137}Cs source at two representative distances, $D = 2$ m and $D = 5$ m, are shown in Fig. 2. Analogous spectra were collected with the source at the other distances listed in Table 1. The peak in the spectra at about bin 115 is due to deposition of the full energy of a 662 keV photon from the ^{137}Cs source. Higher energy peaks, due to naturally occurring U and Th in the concrete structure of the experimental lab, are also apparent in the top two plots.

In the bottom two plots of Fig. 2, the same spectra are shown after live-time normalization and background

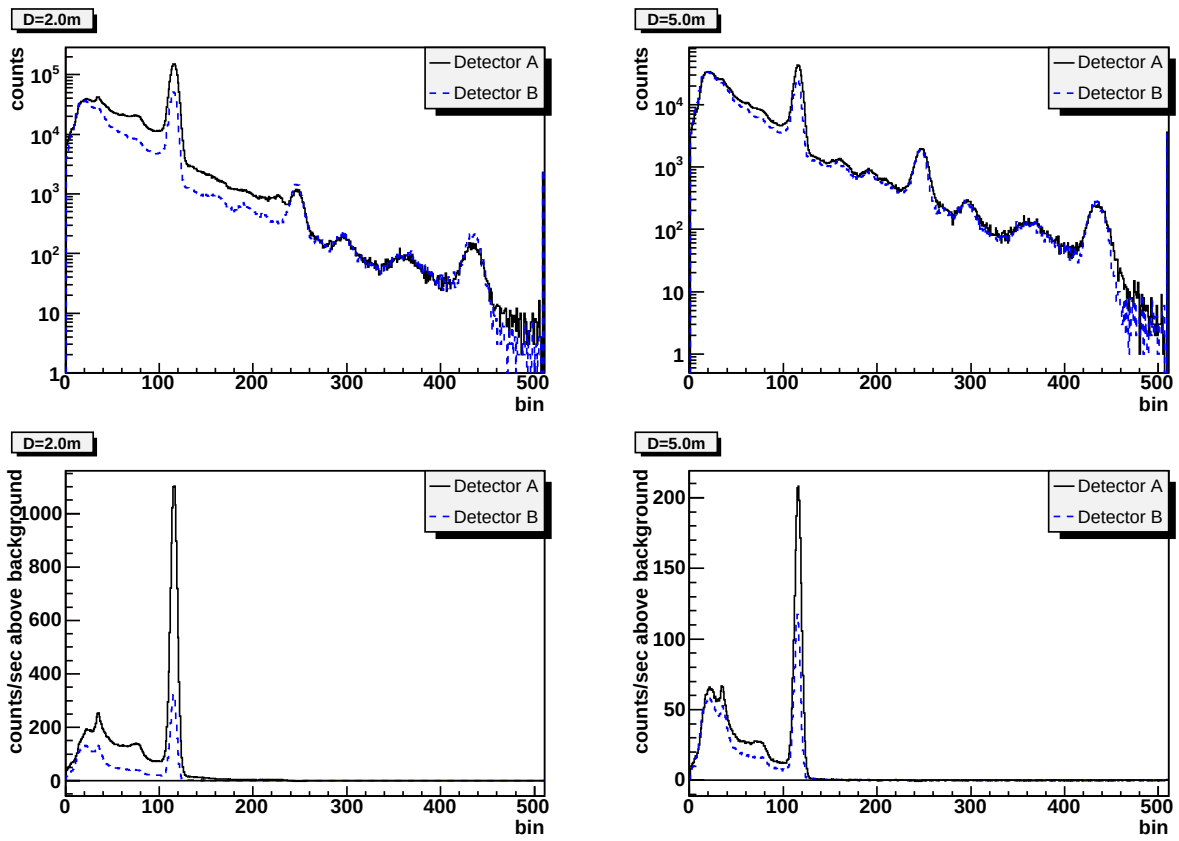

Figure 2: Spectra obtained with ^{137}Cs at $D = 2$ m and at $D = 5$ m. The top two plots show the spectra before background subtraction. The bottom two plots show the spectra after background subtraction. The spectra obtained with Detector A are shown by the solid line and the dashed line shows the spectra obtained with Detector B.

subtraction. The background subtraction reduces the contribution to the spectra above the 662 keV peak to nearly zero everywhere, though the careful eye will observe some evidence of pulse pile-up, about which more in Sec. 5.1.

Detector B, because it is farther from the source, receives a smaller number of ^{137}Cs counts than Detector A. More importantly for the current paper, it is clear by visual inspection of the spectra at the two distances, that the difference between the number of counts obtained by the two detectors is smaller when the source is farther away.

The raw spectra obtained with the ^{60}Co source at the same distances are shown in Fig. 3 (with analogous spectra having been obtained with the ^{60}Co source at the other distances listed in Table 1). Full-energy deposition of the 1173 keV and 1332 keV ^{60}Co photons leads to the two prominent peaks at around bin 200 and bin 225. The background subtraction reduces the counts to numbers consistent with zero above the 1332 keV peak. Again, what is relevant for this study is that the number of counts observed in Detector B is closer to the number of counts observed in Detector A, at the farther of the two source distances.

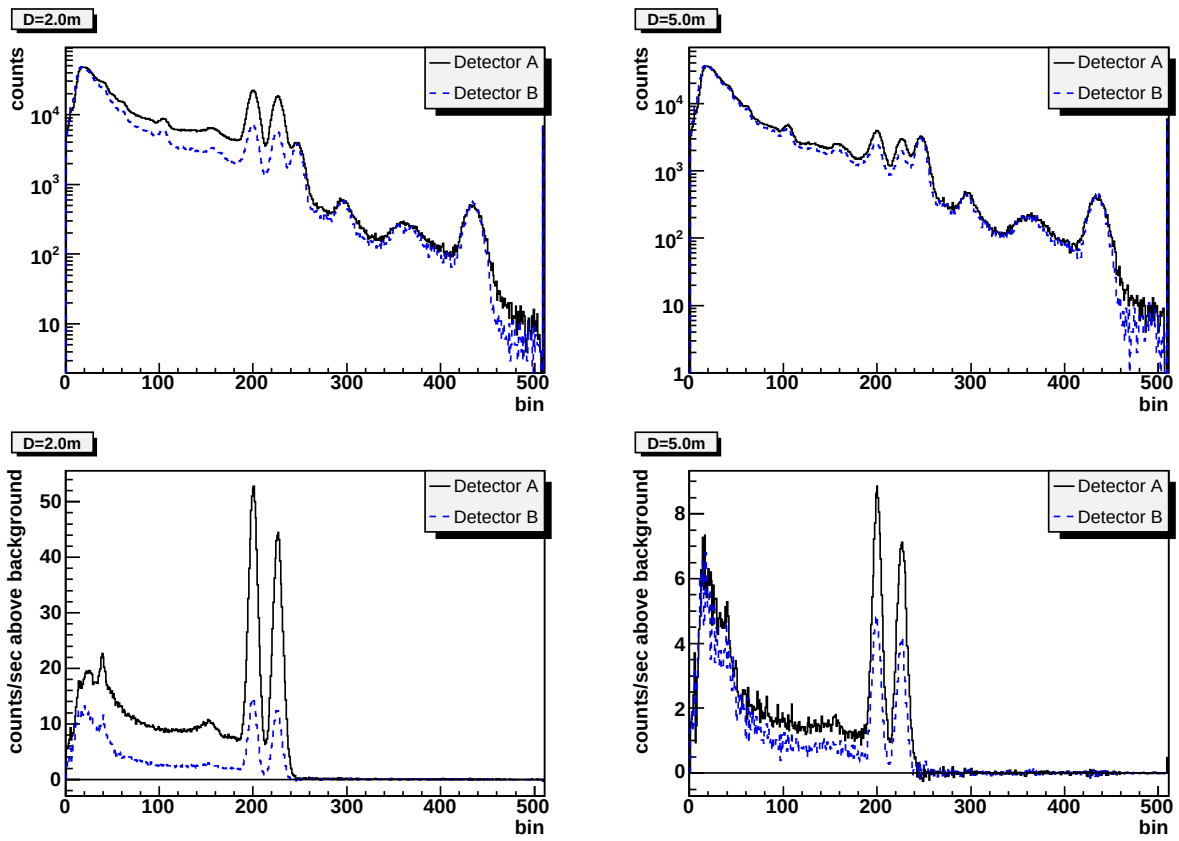

Figure 3: Spectra obtained with ^{60}Co at $D = 2$ m and at $D = 5$ m. The top two plots show the spectra before background subtraction. The bottom two plots show the spectra after background subtraction. The spectra obtained with Detector A are shown by the solid line and the dashed line shows the spectra obtained with Detector B.

5 Analysis

To extract the source distances from the spectra, we first compute the number of counts in the full-energy peak in Detector A (Detector B) after live-time normalization and background subtraction, $C_{\mathrm{A}}^{\mathrm{MEAS}}$ ($C_{\mathrm{B}}^{\mathrm{MEAS}}$). For the analysis of the ^{137}Cs data we have used bins 107 to 125 to compute the peak area and for the analysis of the ^{60}Co data we used bins 215 to 238, corresponding to the 1332 keV peak.

5.1 Pulse pile-up correction

A careful investigation of the spectra reveals the existence of a small pulse pile-up peak at twice the 662 keV full-energy-deposition peak in the data taken with Detector A (the near detector) with the 600 μCi ^{137}Cs source at distances $D \leq 3$ m. The peak can barely be made out in the logarithmic plot of the ^{137}Cs spectra for Detector A at $D = 2$ m which was presented in Fig. 2.

Further evidence of pulse pile-up is the small tail of counts left above the high-energy peak after background-subtraction, shown in the bottom left plot of Fig. 2.

Pulse pile-up leads to a migration of counts out of the full-energy peak, primarily affecting Detector A which

was nearer to the source, and leading to a bias in the ratio $C_{\rm A}^{\rm MEAS}/C_{\rm B}^{\rm MEAS}$. To correct for this effect we have followed a procedure outlined in Ref [5] which we will refer to as the "moving source" pulse pile-up correction. This correction involves determining the resolution time of the spectrometer, τ, by looking at the peak area due to a stationary source, as a function of total count rate, $\mathcal{R}$. We chose as the "stationary source" peak the background peak due to Th. The value of τ has been determined to be $\tau = 3.7 \pm 0.2$ μs. The data have then been corrected for pulse pile-up according to

$$C_{\rm A}^{\rm CORR} = C_{\rm A}^{\rm MEAS} e^{2\mathcal{R}\tau}, \tag{5}$$

and likewise for $C_{\rm B}^{\rm CORR}$. The affect of this correction on the extracted distances is about 10 to 20 cm for data taken with the 600μ Ci source at $D \leq 5$ m, and becoming negligible at larger distances.

5.2 Systematic uncertanties

The central, or "canonical" measurements of the peak areas $C_{\rm A}^{\rm CORR}$ and $C_{\rm B}^{\rm CORR}$ are those obtained using the ^{137}Cs source and applying the moving-source pile-up correction method. To quantify the uncertainty on the measurement of the ratio, $C_{\rm A}^{\rm CORR}/C_{\rm B}^{\rm CORR}$ has been re-computed at $D = 5$ m under a number of alternative conditions.

- We have allowed for uncertainty in the pulse pile-up correction by re-evaluating the peak areas using a simplistic pile-up correction in which we include in the peak area determination, all counts both in and above the peak after background removal.
- The relative count rates in the two detectors would be biased by any anisotropy in the source. To account for this, we repeated the measurement at $D = 5$ m, rotating the ^{137}Cs source to azimuthal positions of 0°, 90°, 180° and 270°.
- Similarly, we allowed for the effect of a polar anisotropy in the source intensity by tilting the cylinder off-vertical by an angle which was judged by eye to correspond to the opening angle between detectors A and B.
- Background subtraction for the "canonical" measurement is performed using the data from a long background run taken at the beginning of the experiment. We allowed for a change in the spectrum of the background radiation by repeating the peak-area calculations, using for the background subtraction data taken toward the end of the experiment, after the ^{137}Cs measurements were complete, and before the ^{60}Co measurements were taken.
- We have repeated the measurement of $C_{\rm A}^{\rm CORR}/C_{\rm B}^{\rm CORR}$ using the ^{60}Co source in place of the ^{137}Cs source.
- Eqn. 4 assumes that the detector acceptances and efficiencies cancel in the ratio $C_{\rm A}/C_{\rm B}$. To quantify the error on the measurement due to incorrectness of this assumption we have repeated the measurement with Detectors A and B swapped.

All variations were consistent with the canonical measurement within statistical fluctuations. An estimate of the systematic uncertainty affecting the ratio was obtained by taking the quadratic sum of the deviations of the alternative measurements from the canonical measurement. This is a conservative estimate, dominated by statistical uncertainties. The relative systematic uncertainty on the ratio is estimated to be 2.70%.

The corrected ratio as a function of source distance, for both the ^{137}Cs runs and the ^{60}Co runs, is shown in Fig 4. The ratio falls dramatically with distance, underscoring the potential to reconstruct source-distance from a measurement of the ratio. The ^{137}Cs and ^{60}Co datasets are in agreement on the dependence of the ratio on distance. Within uncertainties on the measurement, the ratio is adequately described using geometric effects alone, with $R_{\rm B}^2/R_{\rm A}^2$.

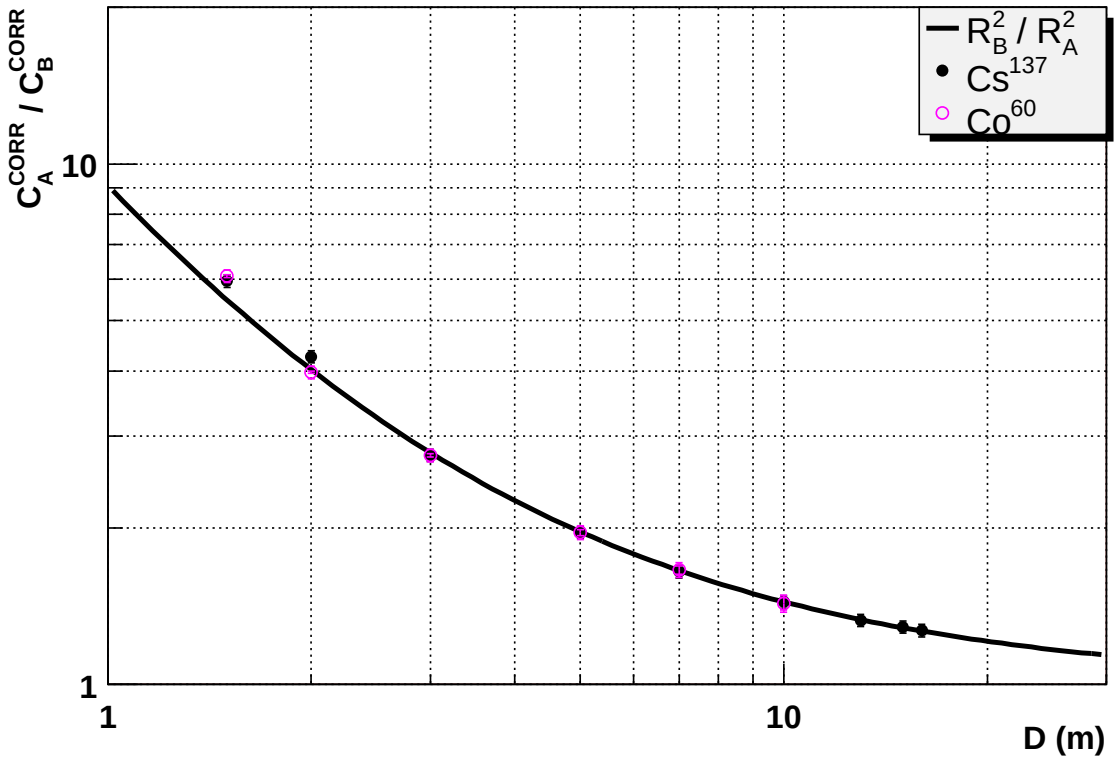

Figure 4: Corrected ratio of peak counts. The filled circles show the ^{137}Cs data and the open circles show the ^{60}Co data. Inner error bars show the statistical errors (not visible on this scale), outer error bars show the quadratic sum of statistical and systematic uncertainties. The curve shows the expectation for the ratio including only geometric effects, $R_{\mathrm{B}}^2/R_{\mathrm{A}}^2$.

5.3 Distance reconstruction

For the current geometry, depicted in Fig. 1, the distance to the source from the front face of the fore detector is $D = R_{\mathrm{A}}$. The horizontal and vertical separations of the two detectors are $d = 2.0$ m and $h = 0.3$ m respectively. Substituting these values into Eqn. 4, the distance D^{REC} can be reconstructed from the measured values of the ratio, $C_{\mathrm{A}}^{\mathrm{CORR}}/C_{\mathrm{B}}^{\mathrm{CORR}}$.

To quantify the systematic uncertainty affecting the distance reconstruction, D^{REC} has been calculated for the canonical measurement, and for each of the aforementioned variations in the experiment which were conducted at $D = 5$ m. The quadratic sum of the deviations of the measurements of D^{REC} from the canonical measurement was taken to be the systematic uncertainty on the measurement of distance. The relative systematic uncertainty on D^{REC} is found in this way to be 4.96%.

6 Results

The reconstructed distances obtained with the 600 μCi ^{137}Cs source (60 μCi ^{60}Co source) are presented in Table 2 (Table 3).

D (m)	$D^{\mathrm{REC}} \pm$ stat. $\pm$ sys.	90% C.L.
1.5	$1.40 \pm 0.00 \pm 0.07$	0.11
2.0	$1.89 \pm 0.01 \pm 0.09$	0.15
3.0	$3.04 \pm 0.01 \pm 0.15$	0.25
5.0	$5.01 \pm 0.03 \pm 0.25$	0.41
7.0	$7.07 \pm 0.06 \pm 0.35$	0.59
10.0	$10.00 \pm 0.13 \pm 0.50$	0.84
13.0	$13.14 \pm 0.28 \pm 0.65$	1.16
15.0	$14.79 \pm 0.39 \pm 0.73$	1.37
16.0	$15.82 \pm 0.48 \pm 0.78$	1.52

Table 2: Measured distances with the ^{137}Cs source, corrected for pulse pile-up, showing statistical and systematic uncertainties separately, as well as the 90% confidence limit.

D (m)	$D^{\mathrm{REC}} \pm$ stat. $\pm$ sys.	90% C.L.
1.5	$1.37 \pm 0.02 \pm 0.07$	0.12
2.0	$2.02 \pm 0.02 \pm 0.10$	0.17
3.0	$3.04 \pm 0.04 \pm 0.15$	0.26
5.0	$5.02 \pm 0.14 \pm 0.25$	0.47
7.0	$6.97 \pm 0.34 \pm 0.35$	0.80
10.0	$10.23 \pm 0.93 \pm 0.51$	1.75

Table 3: Measured distances with the ^{60}Co source, corrected for pulse pile-up, showing statistical and systematic uncertainties separately, as well as the 90% confidence limit.

The reconstructed distances are everywhere consistent, within uncertainties, with the true distances. A clear measure of the usefulness of the method is provided by the 90% confidence limit numbers. Under the idealized conditions of this experiment we find, for instance, that 90% of the time, the distance to a 600 μCi ^{137}Cs source 15 m distant from the front face of the detector arrangement can be reconstructed correctly to within 1.4 m. Likewise, 90% of the time, the distance to a 60 μCi ^{60}Co source at 3.0 m can be reconstructed correctly to within 25 cm.

This same information is presented graphically in Figure 5. The excellent correlation of the reconstructed distances with the true distances is readily apparent.

6.1 Many five-second datasets

A potential application of the gradiometric method presented here would be a truck-borne survey system capable of rapid determination of the location of an off-road source, while the truck is confined to the road. Recall Table 1 which shows the durations of the runs taken to obtain the data presented thus far. Several minutes-worth of data have been used to obtain each distance measurement. For an emergency response application, as much information must be gleaned about the source in the shortest time possible.

We have looked into the potential of the gradiometric method to reconstruct distance given only five seconds of integration time. We divided each dataset into separate five-second samples and reconstructed the source distance several times at each true distance, using as many five-second samples as there were. We thus obtained distributions of D^{REC} at each D. The D^{REC} distributions were approximately Gaussian in shape with a peak at the true D. The widths of Gaussian fits to the D^{REC} distributions were used to assign a statistical uncertainty to the measurement of D^{REC} at each D. (The statistical uncertainties thus obtained were commensurate with the statistical error which would be obtained for five-seconds of data from standard

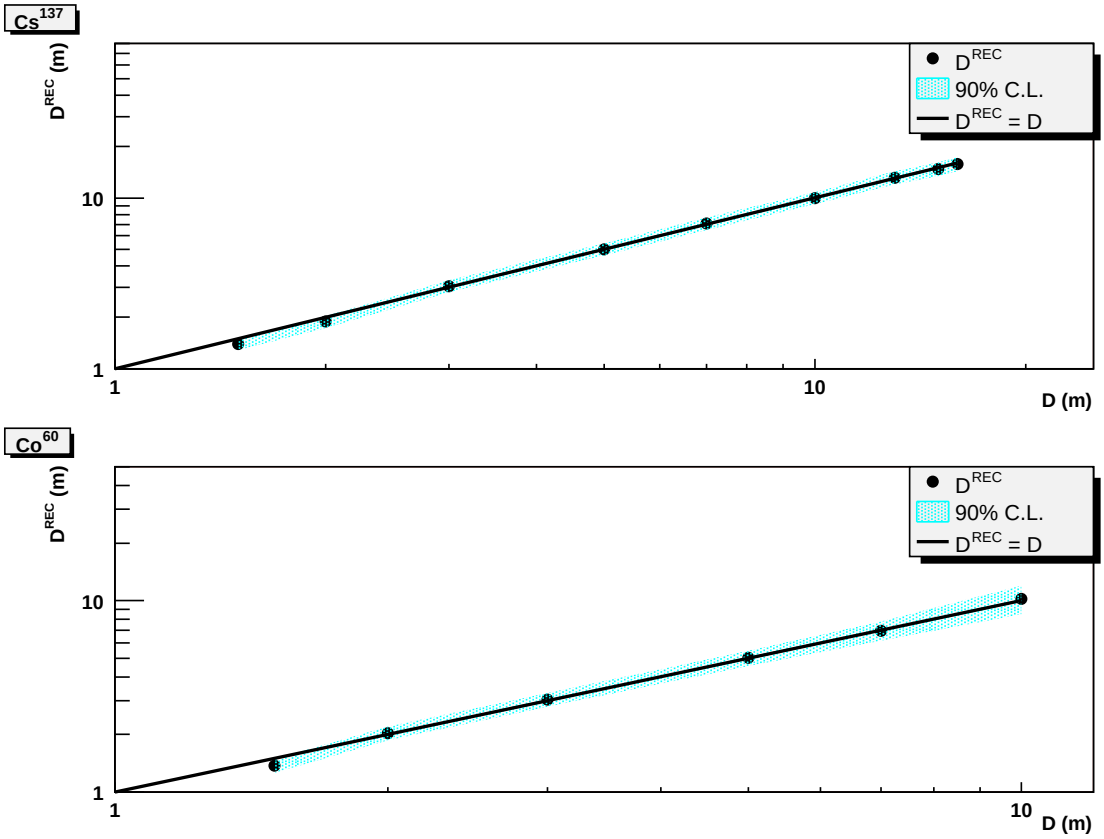

Figure 5: Reconstructed distance as a function of true distance, for all data. Error bars on the data show the combined statistical and systematic uncertainties (not visible). The band shows the 90% confidence limit on the results. The line of D^{REC} equal to D has been drawn.

error propagation.)

The results are shown in Tables 4 and 5, in which the systematic uncertainty obtained from the study of the full dataset presented in Sec. 5.3, has been applied.

The statistical uncertainty of the five-second distance measurements increasingly dominates over the systematic error as distance increases. Distance measurements of useful significance are nevertheless obtained for $D \leq 10$ m with the 600 μCi source, and for $D \leq 3$ m with the 60 μCi source.

The five-second distance measurements are presented graphically in Fig 6. There is a good correlation of the mean of the reconstructed distances with the true distance. The increasing limitation on the method of reconstruction as D increases is illustrated by the widening 90% confidence interval band.

The study of the five-second intervals of data suggests a course of action which could be taken by the survey crew, were the gradiometric method presented here made use of in a truck-borne survey. As the crew drive the road they will notice when they have reached a peak in the count-rate. They pause at that place in the road until enough data has been accumulated and a distance-to-source measurement has been made. This method has the expedient feature for the safety of the crew, that unless the dose-rate is extremely low, an accurate distance measurement will be arrived at in seconds.

D (m)	$D^{\mathrm{REC}} \pm$ stat. $\pm$ sys.	90% C.L.
1.5	$1.65 \pm 0.02 \pm 0.08$	0.14
2.0	$2.14 \pm 0.03 \pm 0.11$	0.18
3.0	$3.26 \pm 0.07 \pm 0.16$	0.29
5.0	$5.22 \pm 0.21 \pm 0.26$	0.55
7.0	$7.28 \pm 0.39 \pm 0.36$	0.88
10.0	$10.34 \pm 1.20 \pm 0.51$	2.15
13.0	$13.37 \pm 2.59 \pm 0.66$	4.40
15.0	$14.75 \pm 4.68 \pm 0.73$	7.80
16.0	$15.69 \pm 3.78 \pm 0.78$	6.35

Table 4: The mean of the distances reconstructed using five seconds of data with the ^{137}Cs source. The width of a Gaussian fit to the distribution of D^{REC} is given as the statistical uncertainty. The systematic uncertainty and the 90% confidence limit are shown.

D (m)	$D^{\mathrm{REC}} \pm$ stat. $\pm$ sys.	90% C.L.
1.5	$1.39 \pm 0.06 \pm 0.07$	0.15
2.0	$2.05 \pm 0.11 \pm 0.10$	0.25
3.0	$3.11 \pm 0.28 \pm 0.15$	0.53
5.0	$4.54 \pm 1.37 \pm 0.23$	2.29
7.0	$6.68 \pm 2.83 \pm 0.33$	4.69
10.0	$6.65 \pm 6.29 \pm 0.33$	10.37

Table 5: The mean of the distances reconstructed using five seconds of data with the ^{60}Co source. The width of a Gaussian fit to the distribution of D^{REC} is given as the statistical uncertainty. The systematic uncertainty and the 90% confidence limit are shown.

6.2 The left side

The gradiometric method of distance determination is also valid when the near detector is the raised detector and the far detector is lower. This geometry would correspond, in the truck-borne scenario we have been imagining, to a source which is on the left-hand side of the road.

We have taken measurements with the 600 μCi ^{137}Cs source at various distances D, with the detectors in the "left-hand side"arrangement depicted in Fig. 7.

Applying the distance-reconstruction method discussed in this paper, we arrive at the reconstructed distances presented in Table 6. The distances are presented with statistical errors only[1].

D (m)	$D^{\mathrm{REC}} \pm$ stat.
1.5	1.93 ± 0.00
2.0	2.15 ± 0.01
3.0	2.97 ± 0.01
5.0	4.69 ± 0.02
10.0	9.25 ± 0.06
15.0	14.65 ± 0.21

Table 6: Measured distances with the ^{137}Cs source on the "left-hand side" of the detector arrangement, corrected for pulse pile-up, showing statistical error only.

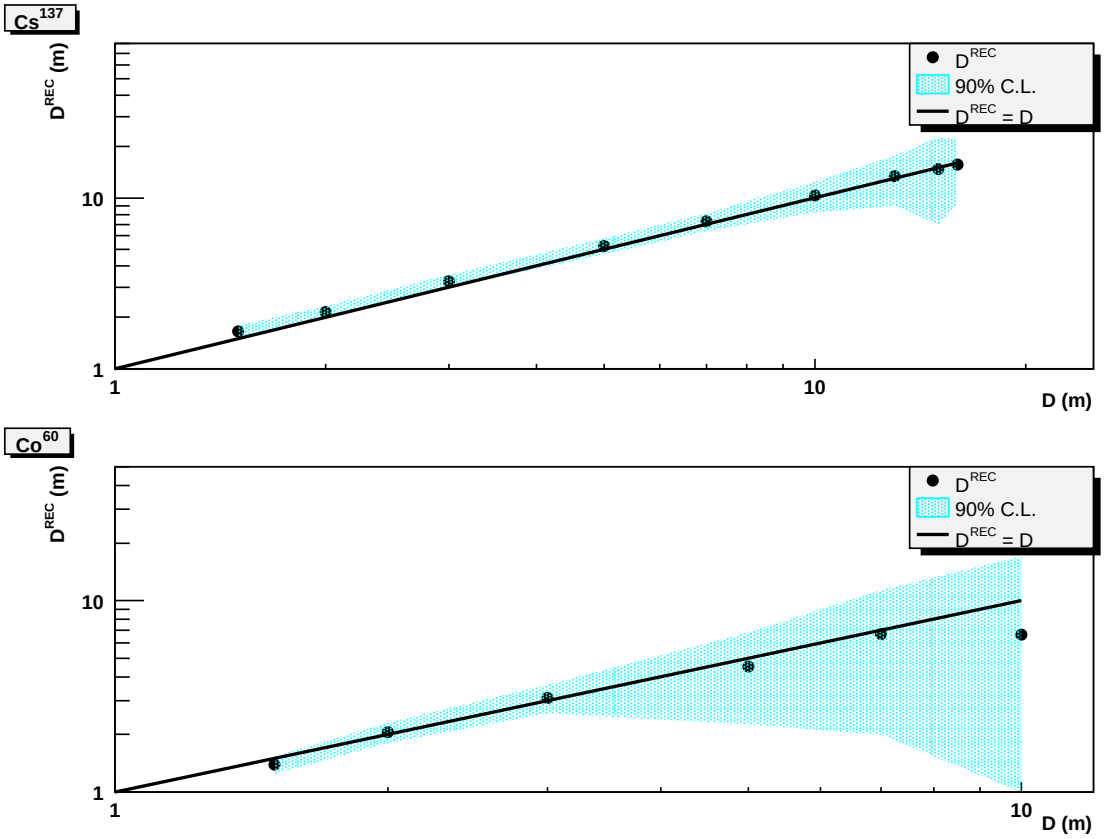

Figure 6: Mean reconstructed distance as a function of true distance, for five seconds of data. The band shows the 90% confidence limit on the results. The line of D^{REC} equal to true distance has been drawn.

Note that the opening angle of the detectors, as seen from the source, is greater in the left-hand side geometry. Uncertainties associated with this effect can be expected to dominate at short distances and are likely the cause of the discrepancy between the measurement and the true distance at $D = 1.5$ m. The agreement with expectations at larger distances is good.

The left-side reconstructed distances are presented graphically in Fig. 8.

Certainly, the data look promising, and indicate that distance measurements on both sides of the detector-arrangement should be possible.

7 Discussion and Conclusions

We have seen that, with a two-detector system under ideal conditions, it is possible to obtain a measure of the distance to a point source which is placed to the side of the two detectors, using a gradiometric method. Several factors could confound the application of this method in a real-life scenario.

In attempting to be as realistic as possible in this demonstration of the gradiometric method, we have used the same number of seconds of background as signal in the computation of each distance. That is, we

[1] We truncate the data at two decimal places, based on our experience with the systematic uncertainties affecting the right-hand side.

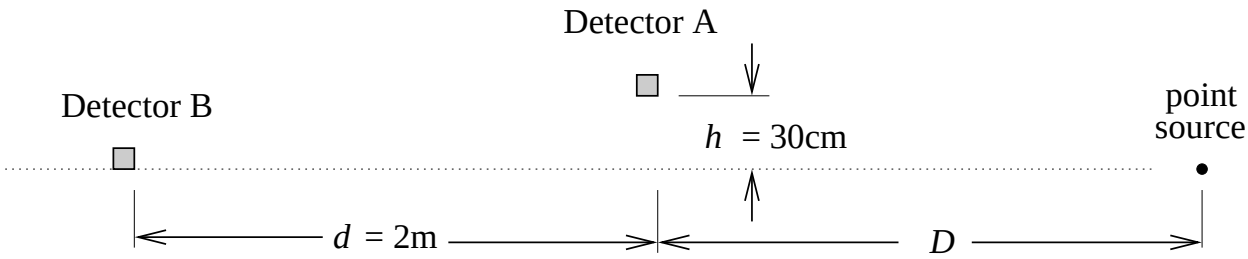

Figure 7: "Left-hand side" experimental setup.

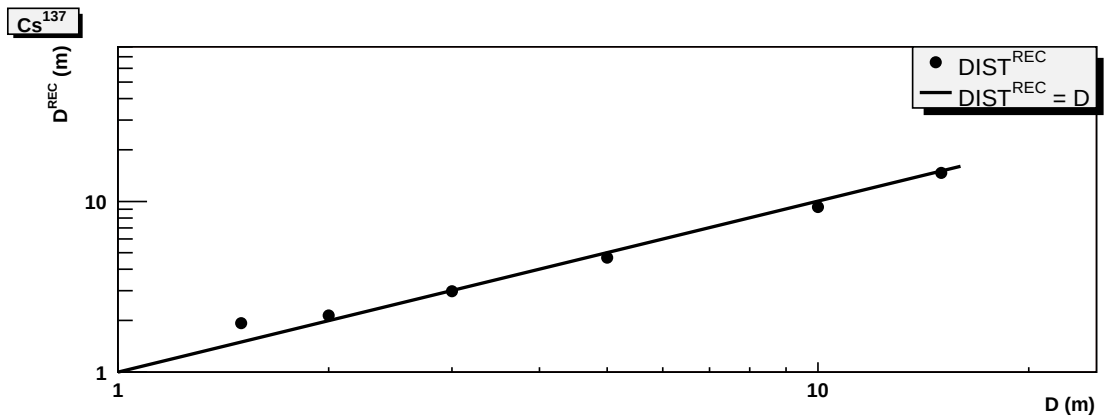

Figure 8: Reconstructed distance as a function of true distance, for left-hand side data. Error bars on the data show the statistical error only (not visible). The line of D^{REC} equal to D has been drawn.

used only five seconds of background data in the five-second distance measurements, so we have a realistic representation of the influence of statistical fluctuations in the background spectrum on the result. There are, however, temporal and geographic variations in background which would affect a truck-borne survey which have not been included in this study. Some additional effort will be necessary to optimize a technique for deducing the shape of the underlying background spectrum from the total spectrum, in real-time.

Note that the presence of uniform shielding between the source and the detectors, such as, for example, a wall, will not throw off the gradiometric method, as this attenuation would cancel in the ratio of peak counts. Non-uniform shielding, however, would present a problem. For example, an obstruction of precisely the right height, situated between the detector-arrangement and the source could shield the lower, near-detector while not shielding the upper detector. This would lead to an overestimate of the distance, or to a reconstructed position on the wrong side of the detector arrangement.

The presence of an extended source, rather than a point source, would also introduce complications into the reconstruction of distance.

Our distance reconstruction method has furthermore assumed that the vertical location of the source is known, i.e. that it is lying on the ground.

The introduction of a third detector into the gradiometric method would provide information which could be used to resolve ambiguities associated with non-uniform shielding and with source shape, and to measure the vertical as well as the horizontal displacement of the source.

We emphasize that the gradiometric method presented in this paper is complementary to an established method by which the distance to a point source is obtained using the change in count rate as a single

detector travels past a source [4]. A system which made use of both methods would have a more powerful handle on source distance, leading ultimately to an improved estimate of source strength, than a system employing either method alone.

In conclusion, we have shown that, using a system of two 4 litre NaI detectors at a relative distance of just over 2 m, it is possible to obtain the distance to a point source up to 15 m distant. The precision of the result depends on the duration of the data-taking. The distance to a 600 μCi source 10 m distant can be resolved in a matter of seconds, while a few minutes of data-taking are required to locate a 60 μCi source at the same distance.

References

[1] International Atomic Energy Agency *Guidelines for radioelement mapping using gamma ray spectrometry data* IAEA-TECDOC-1363 (IAEA, Austria, 2003).

[2] International Atomic Energy Agency *Airborne Gamma Ray Spectrometer Surveying* Technical Reports Series No. 323 (IAEA, Vienna, 1991).

[3] Several field exercises conducted between 2003 and 2006 by the radiological-nuclear laboratory cluster of the federal funding agency CRTI, unpublished.

[4] J. Hovgaard, personal communication.

[5] G. Gilmore and J. Hemingway *Practical Gamma-Ray Spectrometry*, (John Wiley & Sons, Chichester, West Sussex, England, 1995) p. 143.